

DYNAMIC MATERIAL PROPERTIES OF REFRactory MATERIALS: TANTALUM AND TANTALUM/TUNGSTEN ALLOYS

M. D. Furnish¹, D. H. Lassila², L. C. Chhabildas¹ and D. J. Steinberg²

¹Experimental Impact Physics Dept. 1433, Sandia National Laboratories, Albuquerque NM 87185-0821 and

²B-Division, Lawrence Livermore National Laboratory, L-35, P.O. Box 808, Livermore, CA 94551

We have made a careful set of impact wave-profile measurements (16 profiles) on tantalum and tantalum-tungsten alloys at relatively low stresses (to 15 GPa). Alloys used were Ta_{97.5}W_{2.5} and Ta₉₀W₁₀ (wt%) with oxygen contents of 30-70 ppm. Information available from these experiments includes Hugoniot, elastic limits, loading rates, spall strength, unloading paths, reshock structure and specimen thickness effects. Hugoniot and spall properties are illustrated, and are consistent with expectations from earlier work. Modeling the tests with the Steinberg-Lund rate-dependent material model provides for an excellent match of the shape of the plastic wave, although the release wave is not well modeled. There is also a discrepancy between experiments and calculations regarding the relative timing of the elastic and plastic waves that may be due to texture effects.

BACKGROUND

As part of an effort to characterize the viscoplastic behavior of a variety of refractory metals we have undertaken a study of the dynamical properties of molybdenum, tantalum, vanadium and tungsten (all body-centered cubic materials), using time resolved velocity interferometry techniques. The detailed results obtained to date for tungsten, vanadium, tantalum and molybdenum are summarized elsewhere^{1,2,3}. In this paper, the more recent results on tantalum/tungsten alloys are presented. The experiments were conducted over a pressure range of 6.5 to 15 GPa. They were designed to provide waveform data allowing the characterization of yield strengths, shock viscosities, release trajectories and hystereses, and multiwave structures as well as Hugoniot states. These data are then used to evaluate strain-rate-dependent viscoplastic or viscoelastic material models.

The objective of the present paper is to present the data obtained from the experiments conducted with tantalum/tungsten alloys, compare those data with the predictions of hydrocode modeling using candidate viscoelastic and viscoplastic models, and evaluate the success of those models.

MATERIAL SPECIFICATIONS

All materials were forged from bar stock procured from Cabot Corporation. Chemical makeup and densities of the materials are shown in Table 1. Forged material was heat treated in vacuum (10⁻⁷ torr) for one hour, resulting in relatively uniform equiaxed

TABLE 1. Composition and density of samples¹.

Element	Ta	Ta2.5W	Ta10W
Tungsten	15 ppm	3.5 wt%	13.5 wt%
Aluminum	50 ppm	20 ppm	50 ppm
Chromium	10	10	10
Copper	<100	<100	<100
Iron	50	20	50
Magnesium	30	30	30
Nickel	20	<10	20
Titanium	50	50	50
Molybdenum	30	20	30
Tin	50	<10	50
Oxygen	50	30	70
Nitrogen	10	10	10
Carbon	<10	10	35
Co, Mn, Pb, Si, Va	<10	<10	<10
Density (Mg/m ³)	16.696	16.729	16.863

¹In ppm except for W, O, N, H determined by inert gas fusion analysis (LECO); C determined by LECO combustion analysis; all others measured by spectroscopic spark analysis

DISTRIBUTION OF THIS DOCUMENT IS UNLIMITED
Og

MASTER

TABLE 1. Shot conditions and configuration information. Symbols in last column represent sandwich configurations used for tests (materials as noted). All tests included a 6 mm PMMA backer in the projectile.

Test	Target ¹			Projectile ²			■ Sample □ Sapphire ■ Fused Silica	■ PMMA ■ Cu or WC
	Sample 1 (Upper)	Sample 2 (Lower)	Reshock Plate	Impactor	Impact Vel. m/sec			
1	Ta0W (2.332 mm)	Ta10W (2.332 mm)	---	Fused Silica (1.539 mm)	537.5	5 GPa Release	■	■
2	Ta0W (2.250 mm)	Ta2.5W (2.258 mm)	Cu	Fused Silica (1.567 mm)	524.4	5 GPa Reshock	■	■
3	Ta2.5W (2.327 mm)	Ta10W (2.332 mm)	---	Sapphire (3.155 mm)	445.2	11 GPa Release	■	■
4	Ta2.5W (2.324 mm)	Ta10W (2.316 mm)	WC	Sapphire (3.195 mm)	432.4	11 GPa Reshock	■	■
5	Ta0W (2.139 mm)	Ta10W (2.316 mm)	---	Fused Silica (1.560 mm)	844.5	8 GPa Spall	■	■
6	Ta0W (2.241 mm)	Ta2.5W (2.309 mm)	---	Fused Silica (1.577 mm)	827.1	8 GPa Spall	■	■
							■	Projectile Target

1. Targets for tests 1 - 4 included sapphire windows 24 mm thick

2. All projectiles included a 6 mm PMMA backer in back of the reshock plate (where applicable) or the impactor.

recrystallized microstructures with grain sizes in the range of 30 to 60 μm .

EXPERIMENTS CONDUCTED

A total of six impact experiments were conducted, with two samples per experiment. Samples were chosen to allow a comparison of the properties of two different alloys in each test. One velocity interferometer (VISAR)⁴ was used for each sample to measure transmitted wave profiles. Consider the configuration of Figure 1.

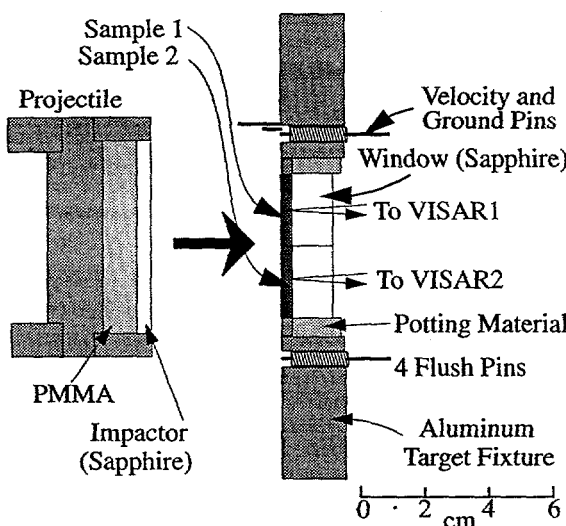


FIGURE 1. Test configuration (Test 3). Other tests similar; see Table 1 for exact components used.

Detailed parameters for the tests are presented in Table 1, including dimensions and configurations.

Upon impact, a compressional wave travels through the samples and into the window. An oppositely directed compressional wave propagates through the flier and reflects from the interface with the PMMA backer as a release wave, which then travels through the samples and into the window. Hence the sample is subjected to a shock followed by a release (a "release" configuration).

Inserting a high-impedance plate between the flier and the PMMA backer causes the sample to experience a shock, a reshock, then a release (a "reshock" configuration). Alternatively, eliminating the sapphire window creates a set of shock interactions which places the sample under dynamic tension, testing spall strength (a "spall" configuration).

Fused silica flier plates were used where stresses would not exceed 8.5 GPa. These have the advantage of providing a rarefaction shock, giving a particularly clean test of sample release behavior. For Tests 3 and 4, however, sapphire was substituted as a flier plate material to circumvent yielding behavior expected in fused silica in the ~11-12 GPa stress region.

VISAR fringe records, which are reduced to give velocity histories at the sample/window interface (or sample free surface, for tests 5 and 6), were acquired on redundant digitizing instrumentation systems. The impact time relative to the digitized traces was

DISCLAIMER

This report was prepared as an account of work sponsored by an agency of the United States Government. Neither the United States Government nor any agency thereof, nor any of their employees, make any warranty, express or implied, or assumes any legal liability or responsibility for the accuracy, completeness, or usefulness of any information, apparatus, product, or process disclosed, or represents that its use would not infringe privately owned rights. Reference herein to any specific commercial product, process, or service by trade name, trademark, manufacturer, or otherwise does not necessarily constitute or imply its endorsement, recommendation, or favoring by the United States Government or any agency thereof. The views and opinions of authors expressed herein do not necessarily state or reflect those of the United States Government or any agency thereof.

DISCLAIMER

**Portions of this document may be illegible
in electronic image products. Images are
produced from the best available original
document.**

calculated from the precursor time-of-arrival, based on ultrasonic measurements of the longitudinal sound velocity in these samples. The resulting velocity histories are shown in Figure 2.

Velocity histories for the first four tests (eight samples) were analyzed by an explicit Lagrangian calculation comparing input and output wave profiles for the sample. This analysis yielded tabular relations between wave speed, stress, strain, strain rate, particle velocity and window velocity. For those experiments with a reshock following the initial shock (2 and 4), this analysis was cut off after the initial shock arrival

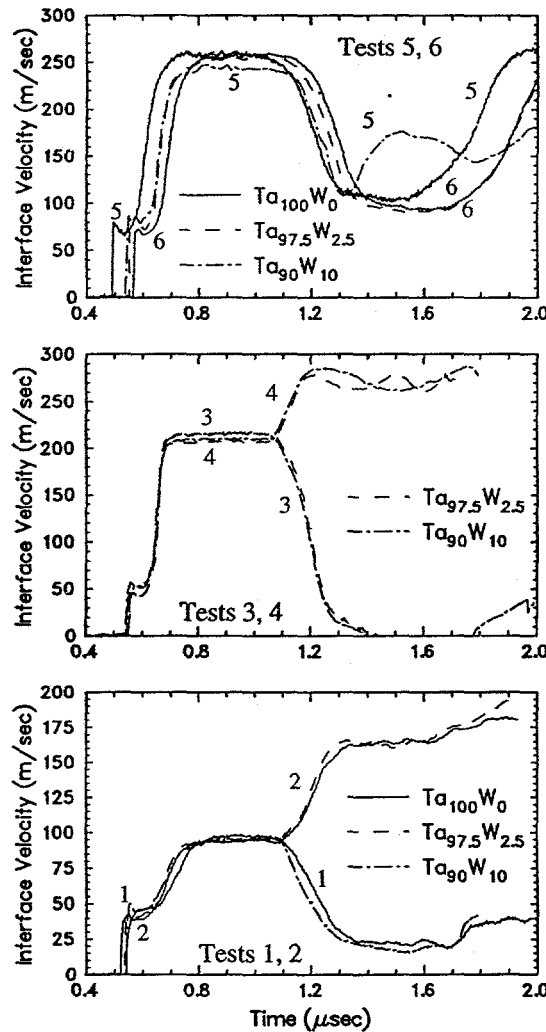


FIGURE 2. Velocity histories for Ta/W tests. Each test includes 2 samples; each plot includes 2 tests (test numbers shown adjacent to waveforms). Compositions are indicated by line style.

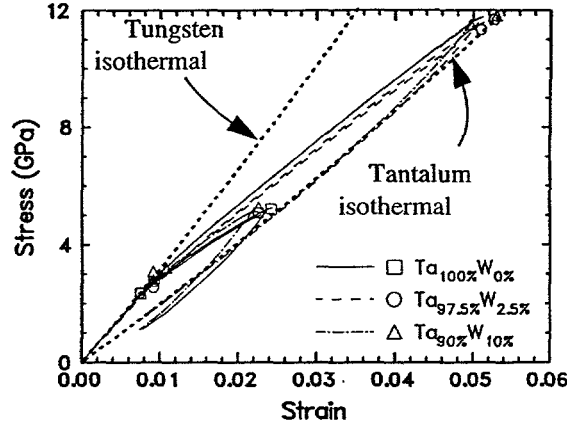


FIGURE 3. Stress vs. strain paths for tests 1 - 4, plotted against Hugoniot and precursor conditions

at the window. Representative results from this analysis are shown in Figure 3.

Precursor and Hugoniot conditions may be calculated directly from impedance match calculations as well. This has been done for the first four tests; the results are plotted in Figure 3.

The tungsten alloying is expected to reduce spall strength in this composition range, based on earlier work utilizing sample recovery techniques⁵. Test 5 gives results consistent with the earlier work, as shown in Figure 4. Here, under identical impact conditions (~5 GPa spall stress following compression to ~8 GPa), pure tungsten did not spall while Ta10W did. No spall was observed in Test 6,

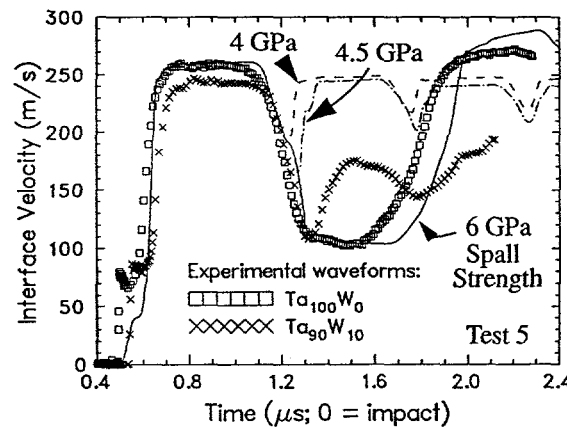


FIGURE 4. Waveforms from Test 5, compared with calculated waveforms for various sample spall strengths.

DISTRIBUTION OF THIS DOCUMENT IS UNLIMITED

which produced similar spall stresses for pure tantalum and Ta2.5W. We emphasize that the present waveform-based observations represent a fundamentally different probe of spall strength than do the earlier observations, which were based on examinations of recovered samples.

SHOCK WAVE PROFILE MODELING

Some of the Ta, Ta2.5W and Ta10W gas gun experiments were simulated using an explicit 1-D computer code, with the samples described by the Steinberg-Guinan-Lund (SGL) rate-dependent model⁷. This model has been shown to be successful in reproducing the strength properties of bcc materials^{1,2,7}. The calculated wave profile for Experiment 3 on Ta2.5W is shown in Figure 5. The SGL parameters used were those of Steinberg and Lund⁷, except that a value of 0.6 GPa was used for the athermal component of the flow stress. The hydrodynamic equation-of-state (EOS) used in the calculations is a Mie-Grüneisen EOS with a linear shock velocity/particle velocity (U_S/U_p) representation⁸. The bulk sound speed, slope and initial density used were 3.41 mm/ μ s, 1.2 and 16.75 gm/cm³, respectively. The shape of the calculated wave profiles is in good agreement with the experimental data. However, the time interval between the arrivals of the elastic precursor and of the so-called plastic wave do not match. This is an elasticity and EOS issue (not related to the SGL

strength model), and was consistent in all of our calculations. In order to obtain good agreement with the experimental data by adjusting EOS parameters, we needed to select unrealistic values, e.g. a slope of 0.75 provided good agreement. Ultrasonic measurements do not explain the issue; Poisson's ratios were 0.364, 0.336 and 0.334 (Ta, Ta2.5W and Ta10W, respectively), which are very close to values from previous work except for Ta (the present value is about 7% higher than the expected value of 0.340). We suggest that this issue may be related to the effects of crystallographic texture (which was undocumented) on wave speed anisotropy.

ACKNOWLEDGEMENTS

This work was performed at Sandia National Laboratories and Lawrence Livermore National Laboratory supported by the U. S. Department of Energy under contract DE-AC04-94AL85000 and others.

REFERENCES

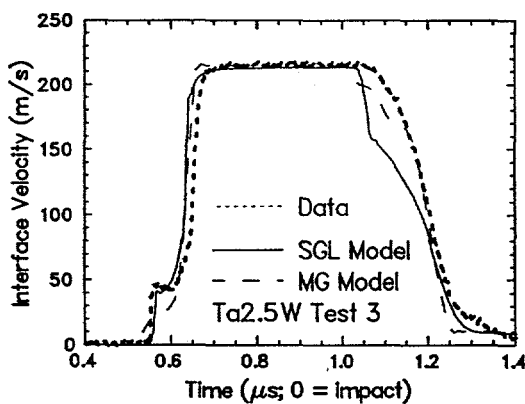


FIGURE 5. Comparison of calculated (SGL and Mie-Grüneisen) and experimental wave profiles for Ta2.5W alloy.

1. M. D. Furnish and L. C. Chhabildas, Dynamical material properties of refractory materials: molybdenum, pp. 229-239 in *High Strain Rate Behavior of Refractory Metals and Alloys*, R. Asfahani, E. Chen and A. Crowson (eds.), TMS, 1992
2. M. D. Furnish, L. C. Chhabildas, D. J. Steinberg and G. T. Gray III, Dynamic behavior of fully dense molybdenum, pp. 419-422 in *Shock Waves in Condensed Matter - 1991*, S. C. Schmidt, R. D. Dick, J. W. Forbes and D. G. Tasker, Elsevier, 1992.
3. L. C. Chhabildas and L. M. Barker, Dynamic quasi-isentropic compression of tungsten, pp. 111-114 in *Shock Waves in Condensed Matter - 1987*, S. C. Schmidt and N. C. Holmes, eds., Elsevier, 1988.
4. L. M. Barker and R. E. Hollenbach, Laser interferometer for measuring high velocities of any reflecting surface, *J. Appl. Phys.*, 43, 4669-4675, 1972.
5. L. Ming and M. H. Manghnani, Isothermal compression of bcc transition metals to 100 kbar, *J. Appl. Phys.*, 49, 208-212, 1978.
6. G. T. Gray III and A. D. Rollett, The high-strain-rate and spallation response of tantalum, Ta-10W and T-111, pp. 303-315 in *High Strain Rate Behavior of Refractory Metals and Alloys*, R. Asfahani, E. Chen and A. Crowson (eds.), TMS, 1992
7. D. J. Steinberg and C. J. Lund, A constitutive model for strain rates from 10^{-4} to 10^6 s⁻¹, *J. Appl. Phys.*, 67, 1991.
8. D. J. Steinberg, Equation of state and strength properties of select materials, Lawrence Livermore National Laboratory Report, UCRL-MA-106439 (1991).